A Switched System Model for Heat Exchangers using a Moving Boundary Method

Thomas L. McKinley, and Andrew G. Alleyne, *Senior Member, IEEE*

Abstract—This paper presents a new switching scheme for moving boundary thermo-fluid models of heat exchangers. Pseudo state variables are introduced to accommodate the changing roles of dynamic variables as the number of different zones is changing. As a result, the number of states is conserved throughout the switches, but the forcing functions of the state derivatives change. A unique switching criteria based on void fraction is introduced and shown to be critical for mass conservation. Simulation results verify both the validity of the switched moving boundary model as well as its usefulness in a system simulation environment.

I. INTRODUCTION

THE moving boundary method [1,2] is one approach to dynamic modeling of heat exchangers that is useful for developing feedback controllers. In this approach, the heat exchanger is divided into zones based on the fluid phase in each region, and model parameters are lumped together in each zone. The location of the boundary between regions is a dynamic variable, thereby capturing the essential two-phase flow dynamics. The resulting models are of low dynamic order, making them very well suited for control design. Furthermore, moving-boundary models provide physical insight into the parametric sensitivity of the plant's dynamic behavior [3]. Additionally, they can be combined with other dynamic component models to create simulations of entire cooling systems that are still amenable to systems analysis and control design [4]. The interested reader is referred to the literature for further details on moving boundary methods, their comparison with other methods [5,6], and their use in control [7-9].

A typical moving boundary heat exchanger model can be formulated in nonlinear descriptor form as [4, 10]:

$$Z(x,u) \cdot \dot{x} = f(x,u) \tag{1}$$

where x is the state vector, containing information about pressures, enthalpies, zone locations and temperature. $f(x,u)$ is a forcing function containing energy balance terms and $Z(x,u)$ is a coefficient matrix containing thermodynamic variables. A key limitation of most moving boundary representations is that the number of zones for a given heat exchanger remains fixed as a function of time [2]. For

T.L. McKinley is with the Department of Mechanical Science and Engineering at the University of Illinois, Urbana-Champaign, 1206 West Green Street, MC-244, Urbana, IL, USA, 61801. (tmckinl2@uiuc.edu)

A. G. Alleyne is with the Department of Mechanical Science and Engineering at the University of Illinois, Urbana Champaign, 1206 West Green Street, MC-244, Urbana, IL, USA, 61801. (phone: 217-244-9993; fax: 217-244-6534; e-mail: alleyne@uiuc.edu).

example, suppose a model is constructed for a condenser in a vapor compression cycle assuming that there is a zone of superheated vapor entering the heat exchanger, a zone of two phase refrigerant, and a zone of sub-cooled liquid leaving the heat exchanger. These three zones then remain as part of the model. Should there be a sudden transient to the system that would cause a loss of sub-cooled liquid, only two zones would be needed to describe the dynamics (two-phase and superheat). Consequently, a conventional moving boundary model would be inadequate. The coefficient matrix, $Z(x,u)$, in (1) would become singular, causing an indeterminate solution to the ODE. This has serious implications for both simulation and control design. For the purposes of the current work, the central limitation to the standard moving boundary formulation is the need to annihilate or create states, x, in (1) when the heat exchanger model switches the number of active zones; e.g. 3-to-2, 2-to-3, 2-to-1, or 1-to-2. In order to overcome this limitation, a novel switched model approach is pursued here.

The field of switched and hybrid systems [11] is a well developed one. There is a wealth of literature on switched controllers [12] as well as switched models, such as stochastic Markov systems [13]. The current work details the framework of a deterministic hybrid moving boundary model that switches between different representations depending on operating conditions as illustrated in Fig 1. The switching criterion is set by the operating conditions of the heat exchanger.
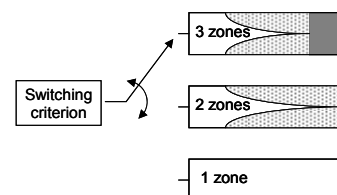

Fig. 1. Schematic of deterministic switching model

The rest of the paper is outlined as follows. Section 2 describes the moving boundary model for a condenser heat exchanger. In particular, Section 2 develops the framework for a 3 zone condenser. Section 3 develops a suitable 2 zone condenser representation lacking a sub-cooled zone. The configurations given in Sections 2 and 3 will be used to demonstrate the switching criterion and method although the concept can be generalized to the other situations shown in Fig 1. Section 4 details the switching approach; in particular, the criterion used as well as the necessary steps to ensure

smoothness of switching as well as conservation of relevant system variables. Section 5 examines the dynamic behavior of the switched model, while Section 6 demonstrates its practical significance in simulating a complete vapor compression cycle system. A conclusion section then summarizes the main results and points out future directions.

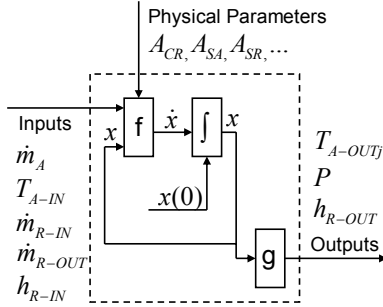## II. 3 ZONE MOVING BOUNDARY MODEL OF A HEAT EXCHANGER

Fig. 2. Schematic of dynamic model and relevant signals.

Fig 2 portrays a schematic of the heat exchanger system in nonlinear state variable form. The time varying inputs are air mass flow rate, air inlet temperature, refrigerant inlet and outlet mass flow rates, and refrigerant inlet enthalpy. The model would be part of a vapor compression cycle simulation [10], so the inputs would be provided by models of other components (e.g. compressors, expansion valves, pipes, junctions). Conditions within the heat exchanger at each instant of time are represented by the following state vector:

$$x = \begin{bmatrix} h_1 & P & h_3 & \zeta_1 & \zeta_2 & T_{W1} & T_{W2} & T_{W3} & \overline{\gamma} \end{bmatrix}^T \quad (2)$$

Model outputs provide an interface to other system components and the user, and can be envisioned as a function (g) of the state vector. Outputs include air outlet temperatures, refrigerant pressure, and outlet refrigerant enthalpy.

To derive functions f and g, the heat exchanger is divided into control volumes or *zones* as shown in Fig 3. The zone size is denoted by the normalized zone lengths $\zeta_i, i \in [1,3]$.

Interface boundaries between zones vary over time and are tracked by the model (hence, the term *moving-boundary method*). As described in the literature [1,2], the governing equations are derived by considering conservation of mass and energy in each control volume. Simplifying assumptions are:

A1. The refrigerant flow is one-dimensional, compressible, and unsteady.
A2. The refrigerant pressure is uniform within the heat exchanger (therefore, the momentum equation is not needed).
A3. Slip flow in the two-phase region can be modeled adequately through a void fraction correlation.
A4. The air entering the condenser has uniform velocity, temperature, and pressure.

A5. The air flow is quasi-steady and incompressible.
A6. Structure internal energy can be adequately represented using a constant specific heat and a single wall temperature for each of the three zones (superheated, two-phase, and sub-cooled).
A7. Conduction along the heat exchanger axis is negligible.
A8. Average air-side and refrigerant-side heat transfer coefficients are adequate to predict heat transfer rates.
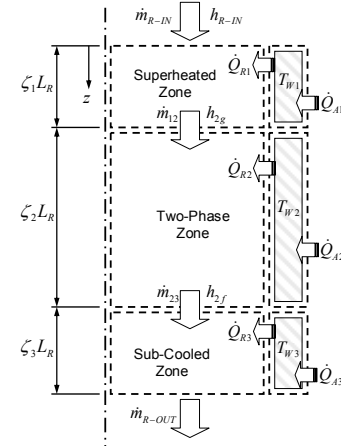

Fig. 3. 3-zone moving boundary model

The following sections describe the governing equations for a cross-flow condenser handling refrigerant and moist air. For this class of heat exchangers, we assume the refrigerant entering the condenser is a superheated vapor. This is a good assumption because the inlet condition to the compressor is usually a superheated vapor and the compression process, with its associated pressure and entropy increase, increases superheat. We also assume some condensation within the condenser such that the outlet condition ranges from a saturated liquid-vapor mixture to a sub-cooled liquid. This is modeled using either a 2 zone (superheated and two-phase zones) or a 3 zone (superheated, two-phase, and sub-cooled zones) representation. Other representations can be derived similarly to the presentation given here.

A. Air Flow Energy Equations

In addition to the assumptions given above, we also assume the specific heat of air is constant and the flow is unmixed. In many applications, the mass and specific heat of the air are much smaller than that of the heat exchanger's metal structure or the refrigerant. Therefore, energy storage in the air can be neglected. Under these constraints, the air temperature profile from inlet to outlet at each instant of time can be derived from the equations for steady, one-dimensional flow. Specifically:

$$T_{A-OUTj} = T_{Wj} + (T_{A-IN} - T_{Wj})\exp[-NTU], \quad j \in [1,3] \quad (3)$$

where:

$$NTU = \frac{\alpha_A A_{SA}[1 - F_{FIN-A}(1-\eta_{FA})]}{\dot{m}_A c_{PA}} \quad (4)$$

The heat transfer rate from the air to the structure, for each zone, can be calculated from:

$$\dot{Q}_{Aj} = \dot{m}_A \zeta_j c_{PA} (T_{A-IN} - T_{A-OUTj}) \tag{5}$$

B. Heat Exchanger Structure Equations

Heat transfer normal to the heat exchanger's z-axis in Fig 2 is caused by air-side and refrigerant-side convection as well as conduction along fins. Since the surface area is many times greater than the cross sectional area, conduction along the length of the heat exchanger can be neglected. Conservation of mass and energy can be combined to derive state equations for the average wall temperature of each zone. For a 3 zone representation:

$$\frac{1}{\zeta_1}\left[\frac{\dot{Q}_{A1} - \dot{Q}_{R1}}{c_W m_W} + (T_{WT1} - T_{W1})\frac{d\zeta_1}{dt}\right] = \frac{dT_{W1}}{dt} \tag{6}$$

$$\frac{1}{\zeta_2}\left[\frac{\dot{Q}_{A2} - \dot{Q}_{R2}}{c_W m_W} + \left(\frac{d\zeta_1}{dt} + \frac{d\zeta_2}{dt}\right)T_{WT2} - \frac{d\zeta_1}{dt}T_{WT1} - T_{W2}\frac{d\zeta_2}{dt}\right] = \frac{dT_{W2}}{dt} \tag{7}$$

$$\frac{1}{\zeta_3}\left[\frac{\dot{Q}_{A3} - \dot{Q}_{R3}}{c_W m_W} + (T_{W3} - T_{WT2})\left(\frac{d\zeta_1}{dt} + \frac{d\zeta_2}{dt}\right)\right] = \frac{dT_{W3}}{dt} \tag{8}$$

Terms containing time derivatives of normalized zone lengths, $d\zeta_i/dt, i \in [1,3]$, represent energy transport due to boundary movement or wall *rezoning*. The temperatures within these terms must be chosen carefully so that energy is conserved on an *integral* basis. That is to say, the time derivative of total wall energy, calculated from the weighted average of wall temperatures for each zone, must equal the total net heat transfer rate into the wall, calculated by summing the net heat transfer rate into each zone. A method ensuring this balance is said to possess the conservative property.

To ensure energy is conserved, the temperature transported between neighboring zones is chosen based on the *interface velocity*. Specifically, when the bottom boundary of a zone moves down in Fig 3, the temperature crossing the boundary is that of the neighboring zone below. Correspondingly, when the bottom boundary moves up, the temperature crossing the boundary is that of the zone itself. In a coordinate system attached to the heat exchanger, normalized interface velocities are:

$$v_{12} = \frac{d\zeta_1}{dt} \tag{9}$$

$$v_{23} = v_{12} + \frac{d\zeta_2}{dt} = \left[\frac{d\zeta_1}{dt} + \frac{d\zeta_2}{dt}\right] \tag{10}$$

Knowing these velocities, temperatures are assigned by:

$$\text{If } v_{12} > 0: \quad T_{WT1} = T_{W2} \tag{11a}$$
$$\text{If } v_{12} \leq 0: \quad T_{WT1} = T_{W1} \tag{11b}$$

$$\text{If } v_{23} > 0: \quad T_{WT2} = T_{W3} \tag{12a}$$
$$\text{If } v_{23} \leq 0: \quad T_{WT2} = T_{W2} \tag{12b}$$

This technique is analogous to the *upwind* or *donor cell* method used in computational fluid dynamics [14]. By summing equations (6) through (8) for arbitrary values of interface velocities, it can be shown that the method possesses the conservative property.

The wall-to-refrigerant heat transfer rate for each zone is computed from:

$$\dot{Q}_{Rj} = \zeta_i U_{Rj} A_{SR} (T_{Wj} - T_{Rj}) \tag{13}$$

Taking into account thermal resistances of the wall and fins, and assuming a uniform heat transfer coefficient over each zone, the overall heat transfer coefficient is given by:

$$U_{Rj} = \frac{1}{\dfrac{t_W}{k_W(1 - F_{FIN-R})} + \dfrac{1}{\alpha_{Rj}[1 - F_{FIN-R}(1 - \eta_{FRj})]}} \tag{14}$$

C. Refrigerant Continuity and Energy Equations

For the superheated zone, the continuity and energy equations are:

$$\frac{d\zeta_1}{dt} + \frac{\zeta_1}{\rho_1}\frac{\partial\rho_1}{\partial P}\frac{dP}{dt} + \frac{\zeta_1}{\rho_1}\frac{\partial\rho_1}{\partial h_1}\frac{dh_1}{dt} + \frac{\dot{m}_{12}}{\rho_1 A_{CR} L_R} = \frac{\dot{m}_{R-IN}}{\rho_1 A_{CR} L_R} \tag{15}$$

$$\frac{dh_1}{dt} - \frac{1}{\rho_1}\frac{dP}{dt} + \frac{(h_g - h_1)}{\rho_1 A_{CR} L_R \zeta_1}\dot{m}_{12} = \frac{\dot{Q}_{R1} + \dot{m}_{R-IN}(h_{R-IN} - h_1)}{\rho_1 A_{CR} L_R \zeta_1} \tag{16}$$

The enthalpy in the superheated zone is given as:

$$h_1 = \frac{h_{R-IN} + h_g}{2} \tag{17}$$

Differentiating Eq. (17) gives:

$$\frac{dh_1}{dt} = \frac{1}{2}\left(\frac{dh_{R-IN}}{dt} + \frac{dh_g}{dt}\right) = \frac{1}{2}\frac{dh_{R-IN}}{dt} + \frac{1}{2}\frac{\partial h_g}{\partial P}\frac{dP}{dt} \tag{18}$$

For the two-phase zone, the continuity and energy equations are:

$$\frac{d\zeta_2}{dt} + \frac{\zeta_2}{\rho_2}\frac{\partial\rho_2}{\partial P}\frac{dP}{dt} + \frac{\dot{m}_{23}}{\rho_2 A_{CR} L_R} - \frac{\dot{m}_{12}}{\rho_2 A_{CR} L_R} + \frac{\zeta_2}{\rho_2}\frac{\partial\rho_2}{\partial\bar{\gamma}}\frac{d\bar{\gamma}}{dt} = 0 \tag{19}$$

$$\left[\frac{\partial h_2}{\partial P} - \frac{1}{\rho_2}\right]\frac{dP}{dt} + \frac{(h_f - h_2)}{\rho_2 A_{CR} L_R \zeta_2}\dot{m}_{23} - \frac{(h_g - h_2)}{\rho_2 A_{CR} L_R \zeta_2}\dot{m}_{12}$$
$$+ \frac{\partial h_2}{\partial\bar{\gamma}}\frac{d\bar{\gamma}}{dt} = \frac{\dot{Q}_{R2}}{\rho_2 A_{CR} L_R \zeta_2} \tag{20}$$

Wedekind [15] pioneered the use of mean void fraction, $\bar{\gamma}$, for lumped parameter models and demonstrated that, for fixed inlet and outlet vapor qualities, the time derivative of this parameter can be neglected [16]. However, for the switching approach described here it is advantageous to include it. Specifically, for the 3 zone representation we establish a first order filter on the difference between $\bar{\gamma}$ and $\bar{\gamma}_{TOT}$, the equilibrium value for complete condensation from saturated vapor to saturated liquid:

$$\frac{d}{dt}(\bar{\gamma} - \bar{\gamma}_{TOT}) = -K_\gamma(\bar{\gamma} - \bar{\gamma}_{TOT}) \tag{21a}$$

$$\Rightarrow \frac{d\bar{\gamma}}{dt} - \frac{\partial\bar{\gamma}_{TOT}}{\partial P}\frac{dP}{dt} = -K_\gamma(\bar{\gamma} - \bar{\gamma}_{TOT}) \tag{21b}$$

Eq (21b) was derived by noting that $\overline{\gamma}_{TOT}$ is a function of pressure. For the simulations of Sections 5 and 6, K_γ was 5.0, which is equivalent to a time constant of 200 ms. This allowed $\overline{\gamma}$ to track changes in $\overline{\gamma}_{TOT}$ with sufficient bandwidth, but in general its value is problem dependent.

For the sub-cooled zone, the continuity and energy equations are:

$$\frac{d\zeta_1}{dt} + \frac{d\zeta_2}{dt} - \frac{(1-\zeta_1-\zeta_2)}{\rho_{3f}}\frac{\partial\rho_3}{\partial h_3}\frac{dh_3}{dt} + \frac{\dot{m}_{23}}{\rho_3 A_{CR} L_R} = \frac{\dot{m}_{R-OUT}}{\rho_3 A_{CR} L_R} \quad (22)$$

$$\frac{dh_3}{dt} - \frac{(h_f - h_3)}{\rho_3 A_{CR} L_R (1-\zeta_1-\zeta_2)}\dot{m}_{23} - \frac{1}{\rho_3}\frac{dP}{dt}$$
$$= \frac{\dot{Q}_{R3}}{\rho_3 A_{CR} L_R (1-\zeta_1-\zeta_2)} \quad (23)$$

In equation (22), the liquid-phase refrigerant was assumed to be incompressible. However, changes in density with enthalpy (thermal expansion) are included.

III. 2 ZONE MOVING BOUNDARY MODEL OF A HEAT EXCHANGER

For the 2 zone moving boundary model, consisting of superheat and two-phase zones, the air-side governing equations are the same as those in Section 2. However, with only 2 active zones, Eq. (3) is replaced by

$$T_{A-OUTj} = T_{Wj} + (T_{A-IN} - T_{Wj})\exp[-NTU], \quad j \in [1,2] \quad (24)$$

where NTU has the same definition as Eq. (4).

A. Heat Exchanger Structure Equations

Equations (6) and (7) still describe the behavior in the first two regions. However, for a 2 zone representation, the sub-cooled zone of the metal structure is not considered to add anything to overall system dynamics. One approach would be to create and annihilate the state T_{W3} when switching between a 2 and 3 zone model. However, that creates fundamental problems for controlling or observing a system based off of that state. Instead, to retain the same number of states independent of the number of zones, Eq (8) is replaced with the following *pseudo state equation*:

$$K_T(T_{W2} - T_{W3}) = \frac{dT_{W3}}{dt} \quad (25)$$

This equation causes the wall temperature for the inactive sub-cooled zone to track the wall temperature of the active two-phase zone. Its function is to provide a reasonable initial condition, should the representation change from 2 zones to 3 zones. Conceptually, it is similar to a latent tracking approach to state or input regulation as would be found in a bumpless transfer controller [17, 18].

B. Refrigerant Continuity and Energy Equations

For the 2 zone representation, Eqs. (15)-(18) still apply to the superheated zone. However, continuity and energy equations for the two-phase zone become:

$$-\frac{d\zeta_1}{dt} + \frac{\zeta_2}{\rho_2}\frac{\partial\rho_2}{\partial P}\frac{dP}{dt} - \frac{\dot{m}_{12}}{\rho_2 A_{CR} L_R} + \frac{\zeta_2}{\rho_2}\frac{\partial\rho_2}{\partial\overline{\gamma}}\frac{d\overline{\gamma}}{dt}$$
$$= -\frac{\dot{m}_{R-OUT}}{\rho_2 A_{CR} L_R} \quad (26)$$

$$\left[\frac{\partial h_2}{\partial P} - \frac{1}{\rho_2}\right]\frac{dP}{dt} - \frac{(h_g - h_2)}{\rho_2 A_{CR} L_R \zeta_2}\dot{m}_{12} + \frac{\partial h_2}{\partial\overline{\gamma}}\frac{d\overline{\gamma}}{dt}$$
$$= \frac{\dot{Q}_{R2} - \dot{m}_{R-OUT}(h_{2-OUT} - h_2)}{\rho_2 A_{CR} L_R \zeta_2} \quad (27)$$

Just as for the structure, we consider the refrigerant's sub-cooled zone to be inactive. Consequently, we assume there are no dynamics associated with the sub-cooled region and therefore:

$$\frac{d\zeta_1}{dt} + \frac{d\zeta_2}{dt} = 0 = \frac{d\zeta_3}{dt} \quad (28)$$

The outlet enthalpy from the two-phase zone in Eq. (27) is determined from pressure and mean void fraction.

In contrast with the 3 zone representation, the time derivative of mean void fraction can be significant in the 2-zone case. However, its value is determined by the aggregation of the continuity and energy equations instead of Eq (21). This is detailed in the following section.

Since the refrigerant sub-cooled zone is inactive, Eqs. (22) and (23) are replaced with the following *pseudo state equation*:

$$\frac{dh_3}{dt} = K_h(h_f - h_3) \quad (29)$$

Eq. (29) forces the enthalpy in the sub-cooled zone to track the saturated liquid enthalpy (h_f), ensuring a reasonable initial condition when the representation changes from 2 zones to 3 zones. As with Eq. (25), the approach in Eq (29) is similar to a latent tracking approach [17, 18] for smooth switching among controllers.

IV. SWITCHING CRITERIA

The pseudo-state equations in (25) and (29) allow the different 2 zone and 3 zone representations to share a common state vector as described in Eqs (1) and (2). Therefore, there is no annihilation or creation of states as the number of zones changes. The only change is the forcing functions for the state derivative equations. This can be stated mathematically as:

$$\dot{x} = Z_{2-ZONE}^{-1}(x,u) f_{2-ZONE}(x,u) \quad (30)$$

for a 2 zone representation, and:

$$\dot{x} = Z_{3-ZONE}^{-1}(x,u) f_{3-ZONE}(x,u) \quad (31)$$

for a 3 zone representation.

Although Eq (31) is the most accurate representation when all three zones are present, as the length of the sub-cooled region approaches zero, certain terms in Eq. (22) and (23) approach zero or infinity. As a consequence, $Z_{3-ZONE}(x,u)$ is no longer invertible. This obstacle can be *prevented* by switching to the 2 zone representation, Eq (30), when sub-cooled zone length is still a small positive

value. The methodology for doing so is given in the following subsections.

A. Switching From 3 Zone to 2 Zone Model

The criteria for switching are based on the normalized length of a particular zone and its time derivative. Specifically, a switch from a 3 to 2 zone representation is triggered when both

$$1 - \zeta_1 - \zeta_2 = \zeta_3 < \zeta_{\min} \qquad (32)$$

and

$$-\frac{d\zeta_1}{dt} - \frac{d\zeta_2}{dt} = \frac{d\zeta_3}{dt} < 0 . \qquad (33)$$

Therefore, switching occurs when the normalized sub-cooled length, ζ_3, falls below some $\zeta_{\min}$ and the time derivative indicates further decrease. The actual value of $\zeta_{\min}$ can be determined by the control designer.

B. Switching From 2 Zone to 3 Zone Model

The criteria for introducing a sub-cooled zone is slightly different from Eqs. (32) and (33). In particular, switching from 2 to 3 zone representation occurs when:

$$\delta\zeta = \zeta_2 \left(\overline{\gamma}_{TOT} - \overline{\gamma} \right) > \zeta_{\min} \qquad (34)$$

and

$$\frac{d\overline{\gamma}}{dt} < 0 . \qquad (35)$$

The value on the left-hand side of Eq (34) is the normalized length of the excess liquid volume. If mean void fraction is below the equilibrium value for complete condensation from saturated vapor to liquid, $\overline{\gamma}_{TOT}$, the term inside parenthesis in Eq. (34) will be positive. This means there is excess liquid volume in the two-phase zone. Eq (35) then indicates that in addition to there being excess liquid in the two-phase zone, there is a positive gradient of liquid accumulation. In Eq (34) the same value of $\zeta_{\min}$ is used as a threshold. This gives the same threshold value when transitioning from 2 zones to 3 zones as when transitioning from 3 zones to 2 zones. However, this is not a requirement for the model and the thresholds could be set differently

C. Switching Symmetry

Sections 4.A and 4.B, and in particular Eqs (32)-(35), indicate that the criteria for switching from 2 to 3 zones are different from the criteria for switching from 3 to 2 zones. This is a function of the framework used for describing the models in Sections 2 and 3. Using Eq (21) in the 3 zone model to track mean void fraction variation, coupled with a switching criteria in Eq. (34), ensures that mean void fraction is continuous through the switching process. Therefore refrigerant mass is conserved. Conservation of mass is critical in moving boundary models because the system response is highly sensitive to mass location and mass flow rates. The next section provides simulation examples to support the choice of switching criteria.

V. SWITCHED CONDENSER SIMULATION RESULTS

The representations developed in Sections 2-4 were tested using a standalone condenser model. Switching performance was checked by holding air and refrigerant inlet conditions constant, but varying refrigerant outlet flow rate harmonically to force repeated switching. Boundary conditions, initial conditions, and physical parameters for this test case are shown in Appendix B.

A. The Need for Continuous States

Fig. 4 shows the sub-cooled zone length and refrigerant pressure for $\zeta_{\min}$ =0.005 with two different versions of the model. Model "A" is consistent with Sections 2-4 and corresponds to the solid lines in this plot. Model "B" is the same as Model "A", except that the algebraic relationship $\overline{\gamma}_{TOT} = \overline{\gamma}_{TOT}(P) = \overline{\gamma}$ was used instead of Eq. (21) for the 3 zone representation. Model "B" results are shown using dashed lines.
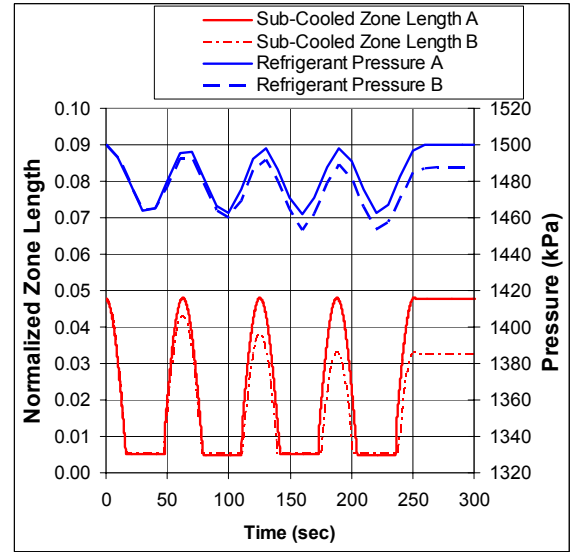

Fig. 4. Simulation Results for a Variation in Refrigerant Outlet Mass Flow Rate. Top graphs are pressure; Bottom Graphs are Normalized Sub-Cooled Length ζ_3

For this periodic input, Model "A" shows the expected periodic variation in zone length and refrigerant pressure. Shortly after switching to a 3 zone representation, zone length transitions to 0.01, since excess liquid volume in the two-phase zone is appended to the sub-cooled zone by the action of Eq (21). For this run, the model switched representations eight times.

Although Model "B" also switches eight times, it shows a fictitious decay in pressure and peak sub-cooled zone length ζ_3. Eq (34) shows that when switching from 2 to 3 zones, void fraction is below the equilibrium value. Failing to retain mean void fraction as a state variable in the 3 zone representation causes it to be discontinuous. This creates a corresponding loss in mass which leads to the erroneous dynamic behavior mentioned above.

This shows the importance of maintaining continuity of states while switching, and all results in the remainder of this paper are with Model "A".

B. Effect of Switching Threshold

Similar runs were made with the switching threshold $\delta\zeta = \zeta_{min}$ varying from 0.01 to 0.0005. Fig 5 shows the corresponding sub-cooled zone length time histories. Although not shown, the threshold did not significantly affect any other predicted values. As expected, reducing the threshold reduced the minimum sub-cooled zone length, and in each case the length always quickly transitioned to twice the threshold when switching from 2 to 3 zones.
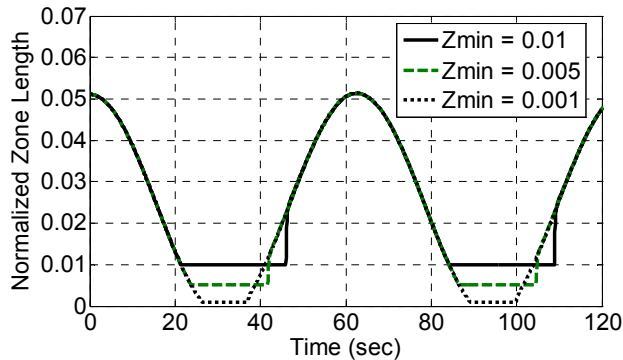

Fig. 5. Impact of Switching Threshold on Sub-Cooled Zone Length Time History (First 120 seconds)

This indicates that the gain in Eq (21) is sufficiently large that, *immediately after the switch from 2 to 3 zones*, terms involving the time derivative of void fraction dominate the governing equations. By noting that liquid density is much larger than vapor densities, and assuming the inactive sub-cooled zone length is ζ_{min}, the following approximation can be derived for this transitional period:

$$\zeta_3 - \zeta_{min} \cong \delta\zeta \left\{1 - \exp[-K_\gamma (t - t_{SWITCH})]\right\} \qquad (36)$$

Table 1. Number of Switches vs Switching Threshold

Switching Threshold $\delta\zeta = \zeta_{min}$	Number of Switches
0.01	8
0.005	8
0.001	14
0.0005	46

Eq (36) violates both criteria for a switch immediately back to 2 zones (Eq (32) and (33)). This *implicit hysteresis* helps avoid repeated switching or *chattering*. However, Table 1 shows that as ζ_{min} is reduced, the number of switches can increase. For this test case, representation switched the expected number of times (eight) for ζ_{min} equal to 0.01 and 0.005. However, $\zeta_{min} = 0.005$ is near a break point where chattering becomes prevalent for the numerical integration scheme used in this work.

VI. TOTAL SYSTEM SIMULATION

The condenser model was also applied in a sample chilled water system using R-134a refrigerant, a water-propylene glycol mixture as a coolant, and moist air as a heat sink. A schematic of the system is shown in Fig. 6, and was modeled using the THERMOSYS MATLAB / SIMULINK toolbox initially developed by Rasmussen [4].
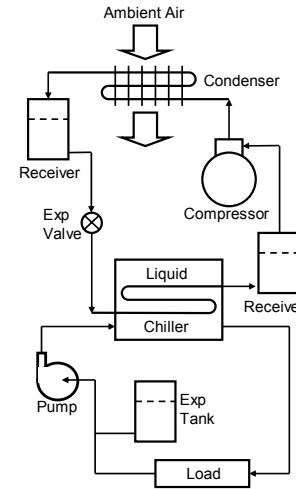

Fig. 6. Sample Simulation System

An electronic expansion valve voltage was varied using a PI controller with feedback on chiller coolant outlet temperature (set point = 11.2 °C). Compressor speed was varied by another PI controller to balance compressor and expansion valve flows. The system was allowed to stabilize for 30 seconds, then chiller load was decreased by 25%. Actuator inputs and system output are shown in Fig. 7.
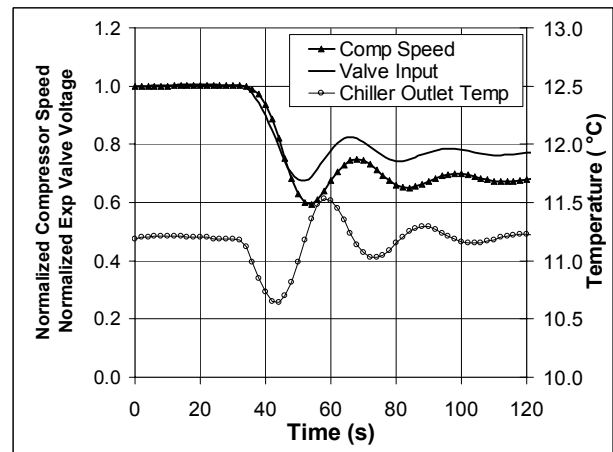

Fig. 7. System Input and Output Response to Load Change

Fig 8 shows normalized zone lengths corresponding to the results in Fig. 7. Normalized sub-cooled zone length peaked at 0.28 near t = 54 seconds. The expansion valve is closing at this time and valve input leads compressor speed input. As a result, more refrigerant is entering and condensing in the condenser than leaves it, and a "plug" of liquid refrigerant forms. To accurately capture this operating

condition, a 3 zone representation is required. Near t = 70 seconds, the sub-cooled region is deactivated. This is due to overshoot in valve and compressor inputs, causing more refrigerant to leave the condenser than is supplied and therefore condensed. As a result, the "plug" of liquid refrigerant is drained away necessitating the use of a 2 zone representation. As can be seen, the switched system model presented here is capable of handling both scenarios.
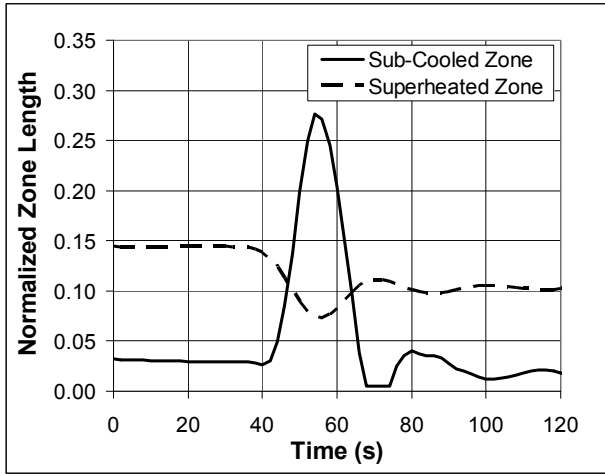

Fig. 8. Zone Length Response to Load Change

VII. CONCLUSION AND FUTURE WORK

This work has developed and demonstrated a moving boundary model accommodating a varying number of zones. Through novel model switching techniques, the range of operating conditions that can be covered was greatly extended. Simulation examples were included to illustrate dynamic behavior when switching and to show the practical need for this capability. Although switching between 2 and 3 zones was the focus of this work, it can also be applied to 1 and 2 zone moving boundary models.

Future work involves the creation of similar modeling procedures for evaporators, receivers, and accumulators. These components are capable of energy storage in vapor compression cycle systems. In addition, complete system models with switched components will be developed.

Both the component and the system models will be validated against detailed experimental data to determine the accuracy and potential gaps in the approach. Prior work has shown agreement within 5% between moving boundary models and test data for steady-state operation [5]. However, further work is needed to quantify their accuracy during transients. Error measures will be based on the most important system outputs (e.g. heat transfer rates and refrigerant outlet conditions).

APPENDIX

A. Nomenclature

A_{CR} Refrigerant cross-sectional (flow) area

A_{SA} Air-to-structure surface area

A_{SR} Refrigerant-to-structure surface area

c_{PA} Air specific heat at constant pressure

c_W Wall (structure) specific heat

F_{FIN-A} Fraction of air-to-structure surface area on fins

F_{FIN-R} Fraction of refrigerant-to-structure surface area on fins

h_j Average refrigerant enthalpy for zone j

h_{R-IN} Inlet refrigerant enthalpy (boundary condition to the model)

h_{R-OUT} Outlet refrigerant enthalpy from the heat exchanger

h_f Refrigerant saturated liquid enthalpy (at pressure P)

h_g Refrigerant saturated vapor enthalpy (at pressure P)

h_{j-OUT} Outlet refrigerant enthalpy from zone j

j Subscript for zone number (1 = superheated, 2 = two-phase, 3 = sub-cooled)

K_h Gain in the enthalpy pseudo state equation; set to 5 s^{-1}

K_T Gain in wall temperature pseudo state eqn; set to 5 s^{-1}

K_γ Gain in mean void fraction pseudo state eqn; set to 5 s^{-1}

k_W Wall thermal conductivity

L_R Refrigerant passage length

$\dot{m}_A$ Air mass flow rate

$\dot{m}_{R-IN}$ Inlet refrigerant mass flow rate

$\dot{m}_{R-OUT}$ Outlet refrigerant mass flow rate

m_W Wall (structure) mass

$\dot{m}_{12}$ Refrigerant mass flow rate from zone 1 to zone 2

$\dot{m}_{23}$ Refrigerant mass flow rate from zone 2 to zone 3

NTU Number of transfer units

P Refrigerant pressure

$\dot{Q}_{Aj}$ Air-to-structure heat transfer rate for zone j

$\dot{Q}_{Rj}$ Structure (Wall)-to-refrigerant heat transfer rate for zone j

T_{A-IN} Inlet air temperature (boundary condition to the model)

T_{A-OUTj} Outlet air temperature for zone j

T_{Rj} Average refrigerant temperature for zone j

T_{Wj} Average wall temperature for zone j

T_{WTj} Wall temperature being transported across the rightmost boundary of zone j due to rezoning

t Time

t_{SWITCH} Time at which a switch occurs

t_W Wall thickness

U_{Rj} Structure (Wall)-to-refrigerant overall heat transfer coefficient for zone j

x State vector

$x(0)$ State vector at time t=0 (initial condition)

$\dot{x}$ Time derivative of the state vector

α_A Average air-side heat transfer coefficient

α_{Rj} Avg refrigerant-side heat transfer coefficient for zone j

$\overline{\gamma}$ Mean void fraction

$\overline{\gamma}_{TOT}$	Equilibrium mean void fraction for complete condensation from saturated vapor to saturated liquid
η_{FA}	Air-side fin efficiency
η_{FRj}	Refrigerant-side fin efficiency for zone j
ζ_j	Fraction of heat exchanger length covered by zone j (also called normalized zone length)
ζ_{min}	Min. normalized zone length before switching occurs
$\delta\zeta$	Normalized length of excess liquid volume in zone 2
ρ_j	Average refrigerant density for zone j
v_{12}	Velocity of the interface between zones 1 and 2
v_{23}	Velocity of the interface between zones 2 and 3

B. Sample Condenser Parameters

Heat Exchanger Type

Flow Arrangement		Cross-Flow	
Pass Arrangement		Single, Un-Mixed	
Construction		Plate-Type	
Boundary Conditions	**Units**	**Air**	**R-134a**
Inlet Flow Rate	kgs^{-1}	1.000	0.060
Inlet Temperature	°C	41	70
Inlet Pressure	kPa	100	1500
Inlet Humidity Ratio	kgkg^{-1}	0.0468	NA
Outlet Mean Flow Rate	kgs^{-1}	1	0.060
Outlet Flow Rate Amplitude (Peak to Peak)	kgs^{-1}	0	0.006
Outlet Flow Rate Frequency	rads^{-1}	0	1
Physical Parameters	**Units**	**Air-Side**	**Ref-Side**
Hydraulic Diameter	mm	2.679	1.149
Passage Length	m	Not Reqd	1.000
Cross-Sectional Area	m^2	8.797E-02	8.775E-04
Total Surface Area	m^2	6.727	2.906
Fin Type	None	Offset Strip Fin	
Fraction of Surface Area on Fins	decimal	0.854	0.659
Fin Thickness	mm	0.102	0.152
Fin Length*	mm	4.763	0.953
Fin Density	fincm^{-1}	5.51	9.45
Fin Offset Length	mm	1.143	3.175
Wall Properties	**Units**		
Mass	kg	3.835	
Thickness	mm	0.406	
Specific Heat	kJkg^{-1}C^{-1}	0.875	
Thermal Conductivity	kWm^{-1}C^{-1}	0.173	

* = Fin length = 1/2*passage height

REFERENCES

[1] E.W. Grald and J.W. MacArthur, "A Moving-Boundary Formulation for Modeling Time-Dependent Two-Phase Flows," *Int J Heat and Fluid Flow*, Vol. 13, No. 3, pp. 266-272, 1992.

[2] M. Willatzen, N.B.O.L. Pettit, and L. Ploug-Sorensen, "A General Dynamic Simulation Model for Evaporators and Condensers in Refrigeration. Part I: Moving-Boundary Formulation of Two-Phase Flows With Heat Exchange," *Int J Refrigeration*, Vol. 21, No. 5, pp. 398-403, 1998.

[3] B. Rasmussen, A. Musser, and A. Alleyne, "Model-Driven System Identification of Transcritical Vapor Compression Systems," *IEEE Trans on Control Systems Technology*, Vol. 13, No. 3, pp. 444-451, 2005.

[4] B. Rasmussen, "Dynamic Modeling and Advanced Control of Air Conditioning and Refrigeration Systems", Ph.D. Thesis, University of Illinois at Urbana-Champaign, 2006.

[5] S. Bendapudi, "Development and Evaluation of Modeling Approaches for Transients in Centrifugal Chillers," Ph.D. Thesis, Purdue University, 2004

[6] S. Bendapudi, J.E. Braun, and E.A. Groll, "Dynamic Model of a Centrifugal Chiller System – Model Development, Numerical Study, and Validation," *ASHRAE Transactions*, Vol. 111, pp. 132-148, 2005.

[7] X.D. He, S. Liu, H. Asada, "Modeling of Vapor Compression Cycles for Multivariable Feedback Control of HVAC Systems," *ASME Journal of Dynamic Systems Measurement & Control*, vol. 119, no. 2, pp. 183-191, June 1997

[8] D. Leducq, J. Guilpart, and G. Trystram, "Low Order Dynamic Model of a Vapor Compression Cycle for Process Control Design," *J of Food Process Engineering*, Vol. 26, pp. 67-91, 2003.

[9] T. Cheng, and H.H. Asada, "Nonlinear Observer Design for a Varying-Order Switched System with Application to Heat Exchangers," *Proceedings of the 2006 Am Control Conf*, Minneapolis, MN, USA, pp. 2898-2903.

[10] A. Alleyne, B. Rasmussen, M. Keir, and B. Eldredge, "Advances in Energy Systems Modeling and Control," *Proc of the 2007 Am Control Conf*; New York, NY USA, pp. 4363-4373..

[11] D. Liberzon, A.S. Morse, "Basic problems in stability and design of switched systems," *IEEE Control Systems Magazine*, Vol. 19, No. 5, 59-70, Oct. 1999.

[12] J. Lygeros, D. N. Godbole, and S. Sastry, "Verified hybrid controllers for automated vehicles," *IEEE Transactions on Automatic Control*, Vol. 43, No. 4, pp. 522--539, 1998

[13] S. P. Meyn, and R.L. Tweedie, Markov Chains and Stochastic Stability, Springer Verlag, 1993.

[14] J.D. Anderson, Computational Fluid Dynamics: the Basics with Applications, McGraw-Hill, NY, pp. 497 ff, 1995.

[15] G.L. Wedekind, B.L. Bhatt, and B.T. Beck, "A System Mean Void Fraction Model for Predicting Various Transient Phenomena Associated With Two-Phase Evaporating and Condensing Flows," *Int. J Multiphase Flow*, Vol. 4, pp. 4, 97-114, 1978.

[16] B.T. Beck, and G.L. Wedekind, "A Generalization of the System Mean Void Fraction Model for Transient Two-Phase Evaporating Flows," *J. of Heat Transfer*, Vol. 103, pp.81-85, 1981.

[17] R. Uram, ''Bumpless Transfer under Digital Control,'' *Control Engineering*, Vol. 18, No. 3, pp. 59–60, 1971.

[18] S.F. Graebe and A. Ahlen, "Bumpless Transfer," in CRC Control Handbook, W.S. Levine Ed., CRC Press, 1996.